Metallomics

PAPER

View Article Online
View Journal | View Issue



Cite this: *Metallomics*, 2015, 7, 662

# Nickel-responsive regulation of two novel *Helicobacter pylori* NikR-targeted genes†

M. D. Jones,[a] I. Ademi,[a] X. Yin,[a] Y. Gong[b] and D. B. Zamble*[a]

Received 7th August 2014,
Accepted 2nd December 2014

DOI: 10.1039/c4mt00210e

www.rsc.org/metallomics

Nickel is an essential transition metal for the survival of *Helicobacter pylori* in the acidic human stomach. The nickel-responsive transcriptional regulator *Hp*NikR is important for maintaining healthy cytosolic nickel concentrations through the regulation of multiple genes, but its complete regulon and role in nickel homeostasis are not well understood. To investigate potential gene targets of *Hp*NikR, ChIP sequencing was performed using *H. pylori* grown at neutral pH in nickel-supplemented media and this experiment identified HPG27_866 (*frpB2*) and HPG27_1499 (*ceuE*). These two genes are annotated to encode a putative iron transporter and a nickel-binding, periplasmic component of an ABC transporter, respectively. *In vitro* DNA-binding assays revealed that *Hp*NikR binds both gene promoter sequences in a nickel-responsive manner with affinities on the order of $\sim 10^{-7}$ M. The recognition sites of *Hp*NikR were identified and loosely correlate with the *Hp*NikR pseudo-consensus sequence (TATTATT-$N_{11}$-AATAATA). Quantitative PCR experiments revealed that HPG27_866 and HPG27_1499 are transcriptionally repressed following growth of *H. pylori* G27 in nickel-supplemented media, and that this response is dependent on *Hp*NikR. In contrast, iron supplementation results in activation of HPG27_1499, but no impact on the expression of HPG27_866 was observed. Metal analysis of the Δ866 strain revealed that HPG27_866 has an impact on nickel accumulation. These studies demonstrate that HPG27_866 and HPG27_1499 are both direct targets of *Hp*NikR and that HPG27_866 influences nickel uptake in *H. pylori*.

## Introduction

The transition metal nickel plays an important role in the survival of many organisms because it serves as a catalytic co-factor for a variety of enzymes.[1–3] A case in point is *H. pylori*, the persistent human pathogen that is estimated to infect 50% of the global population.[4] This microorganism is the causal agent of chronic gastritis, peptic ulcer disease, and gastric mucosa associated lymphoid tissues (MALT) lymphoma, and is the most important risk factor for gastric cancer.[5,6] *H. pylori* are able to survive and thrive under the acidic conditions of the stomach lining, where they encounter pH fluctuations that range from 6 to as low as 1.[7–9] A primary component of *H. pylori* acid defence is the nickel metalloenzyme urease, which generates ammonia and bicarbonate from urea to buffer the cytoplasm and periplasm.[5,10–12] Nickel is also a component of [NiFe]-hydrogenase, an enzyme needed for efficient colonization because it allows *H. pylori* to use the hydrogen gas produced by other host flora as an energy source.[13] Although nickel is a nutritional requirement in this organism and a substantial amount of the metal metabolism of *H. pylori* is devoted to the production of these two obligate nickel enzymes,[14] the metal can be toxic to *H. pylori* if it accumulates inside the cell at high concentrations.[15] Intracellular nickel distribution is tightly controlled in *H. pylori* through the efforts of metalloproteins that function in uptake, efflux, storage, and metalloenzyme assembly.[1,14] Regulation of these metal homeostasis systems is primarily at the transcriptional level, controlled by a nickel-responsive transcription factor called *Hp*NikR.[16,17]

*Hp*NikR is a pleiotropic regulator, acting as either a repressor or an activator of a variety of genes.[16,18,19] Ni(II)-*Hp*NikR regulates transcription upon binding to the promoters of genes that encode factors involved in nickel import (*nixA*, *fecA*, *frpB4*, *exbB*), nickel storage (*hpn*), enzymatic activity (*ureAB*), autoregulation (*nikR*), as well as genes involved in iron homeostasis (*fur*, *pfr*) and possibly other cellular processes.[18,20–23] *Hp*NikR is also involved in the global response of *H. pylori* to acidic conditions,[24,25] and there is evidence that the activity of *Hp*NikR is directly modulated by changes in pH.[21] The mechanism by which nickel or protons activate DNA binding by *Hp*NikR remains unresolved.[20,21,24,26,27] Furthermore, a strong consensus DNA-binding sequence for *Hp*NikR has not been identified. Several iterations of alignments of the DNA recognition

[a] Department of Chemistry, University of Toronto, 80 St. George St., Toronto, ON, M5S 3H6, Canada. E-mail: dzamble@chem.utoronto.ca
[b] Department of Cell and Systems Biology, the Centre for the Analysis of Genome Evolution and Function, University of Toronto, Canada

† Electronic supplementary information (ESI) available: Primer sequences, ChIP-Seq peak targets, additional DNA assay gels and qPCR data. See DOI: 10.1039/c4mt00210e

sites on multiple *Hp*NikR target promoters highlighted an A/T-rich pseudo-palindromic recognition sequence,[28,29] with varying degrees of conservation observed. Furthermore, less sequence conservation correlates with weaker binding *in vitro*,[20] suggesting a mechanism of hierarchical regulation. However, several *Hp*NikR-controlled genes have been identified that lack any sequence homology with the proposed consensus,[22] consistent with a more complicated strategy for DNA recognition by *Hp*NikR.[30]

Understanding the complete physiological function of *Hp*NikR requires that all of the *Hp*NikR targets be identified. To this end, we performed a chromatin immunoprecipitation experiment followed by sequencing (ChIP-seq), which revealed the promoters of HPG27_866 and HPG27_1499. HPG27_866 encodes FrpB2, a putative iron-responsive outer membrane protein,[31–33] whereas HPG27_1499 encodes the *H. pylori* homolog of CeuE, the periplasmic binding protein (PBP) component of an ABC transporter that has been associated with iron networks and more recently with nickel uptake.[33–35] Neither of these genes were a part of the defined *Hp*NikR regulon, but given the association of both gene products with metal homeostasis, we examined whether they were under the control of *Hp*NikR. To validate these genes as *Hp*NikR targets, DNA binding to the promoter sequences by *Hp*NikR was investigated *in vitro*. Purified *Hp*NikR binds to both DNA sequences in a nickel-dependent manner, and the recognition sites were mapped out. Analysis of transcription in *H. pylori* revealed that both genes are repressed upon supplementation of the growth media with nickel and that this response is dependent on *Hp*NikR. In contrast to a previous report,[32] iron-responsive regulation of HPG27_866 was not observed in this study, but upregulation of HPG27_1499 was detected. Furthermore, deletion of HPG27_866 revealed that the gene product has an impact on nickel uptake. These results provide insight into the role of *Hp*NikR as a global regulator of multiple genes in *H. pylori* and the *Hp*NikR mechanism of action in nickel homeostasis.

# Experimental

### Bacterial strains and vector construction

The *ΔnikR H. pylori* G27 strain was generously donated by Dr Peter Chivers (School of Biological and Biomedical Sciences, Durham University, UK).[36] The pET24bhpnikr vector was generated previously.[37] The promoters of 866 and 1499 were PCR amplified from the G27 genome by using the p866F/p866R and p1499F/p1499R primers, respectively (see Table S1 (ESI†) for primer sequences) and inserted into a pBS-SK(+) vector following digestion with the *EagI* and *SalI* restriction enzymes.

### Protein expression and purification

The pET24bhpnikr plasmid bearing the *Hp*NikR gene was transformed into BL21(DE3) Star *E. coli* cells and expressed and purified as previously described.[37] Briefly, the bacteria were grown in LB media containing 50 μg ml$^{-1}$ kanamycin to an optical density of 0.8–0.9 at 600 nm ($OD_{600}$) and protein expression was induced with 0.3 mM isopropyl-β-D-thiogalactopyranoside (IPTG) at 15 °C for 4 hours. The cells were then lysed *via* sonication in protein buffer (20 mM Tris, pH 7.6 and 100 mM NaCl) and centrifuged at 36 000*g* for 1 hour at 4 °C. *Hp*NikR was purified from the supernatant by using Ni-NTA resin followed by dialysis in protein buffer containing 10 mM EDTA and 2 mM DTT. The dialyzed protein was further purified by anion exchange chromatography on a UnoQ column (Bio-Rad) run with a NaCl gradient in 20 mM Tris, pH 7.6, and the protein eluted at approximately 200 mM NaCl. Fractions containing protein were identified *via* 12% SDS-PAGE, concentrated, and stored at 4 °C. *Hp*NikR concentration was determined using electronic absorption spectroscopy with a predicted extinction coefficient of 8480 M$^{-1}$ cm$^{-1}$ at 280 nm and the oxidation state of the protein was detected by performing a 5,5′-dithiobis-(2-nitrobenzoic acid) (DTNB) assay as previously described.[37] Only protein that was >90% reduced was used.

### Electrophoretic mobility shift assays

The 194 bp DNA probes containing the sequences from the 866 and 1499 promoters were PCR amplified from their respective pBS plasmids by using the p866F/p866R and p1499F/p1499R primers, respectively (Table S1, ESI†). The DNA radiolabeling and mobility shift assay experiments were performed as described previously.[37] The samples were resolved on 6% native polyacrylamide gels prepared with Tris-borate (TB) containing either 800 μM $NiSO_4$, 3 mM $MgSO_4$, or 1 mM EDTA in TB running buffer supplemented with the same amount of metal or chelator. The gels were dried and exposed overnight to a phosphor screen, scanned with Pharos FX Plus Molecular Imager (BioRad) and analysed using Quantity One software. The fraction of DNA bound was determined by measuring the intensity of the bound DNA divided by the total intensity of the overall lane. Data were fitted to a Hill equation: $r = [Hp\text{NikR}]^n/((K_{d\,app})^n + [Hp\text{NikR}]^n)$ where $r$ is the fraction of DNA bound to protein and $K_{d\,app}$ is the protein concentration required for 50% DNA binding.

### DNase I footprinting assays

DNA probes of the 866 and 1499 promoters were radiolabeled as described above. To achieve single-strand labelling, the 5′ ends of the labelled oligonucleotides were cut with *SalI*, generating 185 bp and 179 bp probes, respectively. To remove the 5′ fragment, the DNA probes were resolved on a 7% native polyacrylamide gel, and the DNA was eluted from the gel piece by electro-dialysis at 100 V for 2 hours and then precipitated with ethanol at −20 °C. The amount of labelled probe was quantified by liquid scintillation counting on a Tri-Carb Scintillation Counter (Packard). To localize the footprint and confirm that the correct DNA sequence was obtained, the Maxam–Gilbert reaction for guanine bases was performed as described.[38,39]

Increasing concentrations of holo-*Hp*NikR were incubated for 1 hour at room temperature with the radiolabeled promoters in DNase binding buffer (100 mM KCl, 20 mM Tris-HCl, pH 7.6, 1 mM $MgCl_2$, 1 mM $CaCl_2$ and 0.5% (v/v) glycerol and

0.01% IGEPAL). Following incubation, 1 μL of 0.4 U of an RNase-free DNase I enzyme (Invitrogen) was added to each 20 μL sample and quenched after 4 min at room temperature by the addition of 80 μL DNase stop buffer (20 mM Tris, pH 8, 40 mM EDTA, 1% (w/v) SDS, 0.1 μg $\mu L^{-1}$ herring sperm DNA). The proteins were extracted from the samples by using a 24 : 25 : 1 phenol : chloroform : isoamyl alcohol mixture and the DNA was precipitated with ethanol at −20 °C overnight. The samples were then centrifuged, and the DNA was resuspended in 4 μL formamide loading dye and denatured at 90 °C for 3 min before loading onto a pre-run 8% denaturing polyacrylamide gel. The samples were then resolved at 1700 V for 2 hours in TBE buffer (89 mM Tris-HCl, pH 7.5, 87 mM borate and 20 mM EDTA). The gel was vacuum-dried and exposed overnight to a phosphor screen, scanned with a Pharos FX Plus Molecular Imager (Bio-Rad) and analysed using Quantity One software. The degree of protection was determined by quantifying the intensity of 2 bands within the recognition sequence relative to a reference band. Half maximal binding was calculated by fitting the data to the Hill equation with a variable Hill coefficient as described for the electrophoretic mobility shift assays.

### *H. pylori* growth conditions and nickel exposure

Wild-type *H. pylori* G27 and its isogenic *ΔnikR* strain were plated on Columbia agar plates containing 5% horse blood (Thermo Scientific) under a microaerobic environment (5% $O_2$, 10% $CO_2$ and 85% $N_2$) at 37 °C for two days, then replated on new Columbia blood agar plates and grown for a further 22 hours. The colonies were then cultured in 30 mL of Brucella broth with 10% fetal bovine serum (Gibco BRL) and 25 μg $mL^{-1}$ Helicobacter Selective Supplement (Oxoid) while shaking at 100 rpm at 37 °C under the microaerobic environment for 10–15 hours up to an $OD_{600}$ of 0.5–0.7. For overnight exposure to nickel, the medium was supplemented with 10 μM $NiCl_2$. Samples for qPCR from the overnight exposure were collected by pelleting an aliquot of the cells such that the final number of bacteria per sample was $\sim 4 \times 10^7$. For transient nickel exposure, *H. pylori* grown overnight without added nickel were transferred to 5 mL of fresh Brucella broth at pH 7.0 to a final $OD_{600}$ of 0.2, supplemented with 50 mM urea and with or without 100 μM $NiCl_2$. The cells were incubated for 15 minutes at 37 °C in a microaerobic environment and then pelleted at 4000 rpm at 4 °C for 10 minutes. The supernatant was removed using a vacuum pump and the pellets were either immediately stored at −80 °C or lysed for RNA isolation. After the exposure but prior to centrifugation, 10 μL aliquots of the cultures were collected and serially diluted ten-fold in Brucella broth three times. An aliquot of 5 μM from each dilution was spotted on a Columbia blood agar plate and incubated for 3 days to measure cell viability.

### Chromatin immunoprecipitation

The *Helicobacter pylori* strain G27 was grown as a liquid culture at pH 7.0 supplemented with 20 μM $NiCl_2$ as described above. The ChIP experiment was carried out using the One-Day Chromatin Immunoprecipitation Kit (Millipore), with a bacterial sample size of $2 \times 10^8$ cells and five thirty-second pulses in a bath sonicator to lyse the cells and shear the DNA to an average fragment size of 200–500 bp. The remainder of the protocol was as prescribed by the kit. Rabbit polyclonal anti-*Hp*NikR antibody (raised against purified *Hp*NikR, Division of Comparative Medicine, University of Toronto) was purified from serum by Western blotting using purified *Hp*NikR protein as previously described.[40] The recovered genomic DNA was sequenced by Illumina sequencing at ACTG Corporation (Toronto, ON). The reads for ChIP and control DNA isolated with IgG were 35 284 339 and 39 211 483, respectively. The reads were aligned to the *H. pylori* G27 genomic DNA sequence using the Novoalign short sequence alignment software (novocraft.com). The location information of uniquely mapped reads was converted to BED (Browser Extensible Data) format and used as input for the peak finding software SISSRs (Site Identification from Short Sequence Reads).[41] SISSRs was run for binding site identification with the parameters $D = 0.001, 0.01, 0.1$; $e = 1, 5, 10$; $p = 0.1, 0.01, 0.001$ and $w = 2, 4, 8, 16$. A php script was used to merge the identified sequences. These hits were matched with promoters for various genes in *H. pylori* G27 and used to generate a list of potential regulation targets of *Hp*NikR.

### *H. pylori* knockout construction

To generate a knockout of the HPG27_866 gene in *H. pylori* G27, a DNA construct containing the *aphA-3* kanamycin resistance cassette from *Campylobacter coli* flanked by two homological regions corresponding to the 500 bases upstream and downstream of the HPG27_866 gene was synthesized (BioBasic Canada, Inc.). The construct was transformed into wild-type *H. pylori* G27 *via* natural transformation, as previously described.[42] Briefly, a lawn of *H. pylori* was collected from a Columbia blood agar plate grown for two days, resuspended in Brucella broth, spotted onto another blood agar plate and incubated under microaerophilic conditions at 37 °C for 4 hours. At that point, 2 μg of the knockout construct DNA was applied to the spot, given time to dry and then further incubated for 12 hours. The spot was then resuspended in Brucella broth and plated onto blood agar plates containing 50 μg $mL^{-1}$ kanamycin. Colonies of transformants were collected after 3 days. Successful incorporation of the resistance cassette was checked by amplifying the genomic DNA of the transformants around the HPG27_866 gene by PCR using the primers sKO866_F and sKO866_R (Table S1, ESI†). The upstream and downstream junctions of the recombination region were also amplified using the primers sKO866up_F, sKO866up_R, sKO866dwn_F and sKO866dwn_R (Table S1, ESI†) and the products were sequenced to ensure that the genes flanking the *aphA-3* cassette were not disrupted.

### RNA isolation and reverse transcription

*H. pylori* G27 RNA was isolated by resuspending and lysing the bacterial pellet for 5 min in 1 mL of the TRIzol reagent (Invitrogen), according to product protocols. The aqueous layer extracted from the TRIzol was washed twice with chloroform and the RNA precipitated with isopropanol for at least 2 hours at −20 °C. The RNA was then pelleted and washed with 70%

ethanol. The resulting RNA pellet was air-dried, resuspended in 30 μL DEPC-treated water and treated with 178 U of RNase-free DNase I (Invitrogen) to remove trace genomic DNA. The crude RNA was then further cleaned using Aurum Total RNA Mini Kit (Bio-Rad). Purified RNA was quantified using an ND-1000 Nanodrop spectrophotometer and analysed using 1.5% agarose gel electrophoresis to monitor RNA integrity. Only RNA with an $A_{260}/A_{280}$ ratio greater than 1.8 was used for reverse transcription. RNA from each condition was then diluted to 50 ng $\mu L^{-1}$ and converted to cDNA using the iScript cDNA Synthesis Kit (Bio-Rad) according to product protocol with 500 ng of RNA as the template. The remaining RNA was stored at −80 °C and the cDNA was stored at −20 °C.

### Quantitative PCR

All quantitative PCR was performed by using a CFX96 Real-Time System (Bio-Rad) with SsoFast Master Mix (Bio-Rad). Samples were prepared according to the product protocols, with 400 nM combined primer concentration per well. The q16Sf/r, qgyrf/r, qUreAf/r, q866f/r and q1499f/r primers were used to monitor the expression of 16S rRNA, *gyr*, *ureA*, 866 and 1499 transcripts, respectively (Table S1, ESI†). The optimal primer annealing temperature of 55 °C was determined through temperature gradient qPCR and all primers used gave efficiency values between 90 and 110%. All experiments were performed with 45 cycles of a two-step program (5 seconds at 95 °C, 10 seconds at 55 °C) in technical triplicate for at least three biological replicates. A melting curve was also measured at the end of the reaction to ensure the specificity of each primer. The relative expression of the target genes was normalized to the *16S* rRNA and *gyr* levels for each condition and then relative to expression in wild type *H. pylori* in the absence of nickel. The mRNA expression levels of *rpoA* were also examined as a possible reference gene, but its expression was not sufficiently constant under the investigated conditions to be included in these studies (data not shown). Compared to alternate housekeeping genes, 16S and *gyr* expression produced the smallest combined coefficient of variation ($<0.25$) and M value ($<0.5$) as calculated by geNorm (BioRad) (data not shown). No-template controls (NTC) and no-reverse transcriptase controls (NRT) were also run for each primer pair to confirm the lack of primer–dimer formation/DNA contamination and genomic DNA contamination, respectively.

### Inductively coupled plasma mass spectrometry

All ICP-MS experiments were performed on a Sciex ELAN 6100 ICP Mass Spectrometer (Perkin Elmer). Overnight cell samples grown in media with and without 10 μM supplemented nickel (as described above) were collected by spinning down an aliquot of cells such that the final $OD_{600}$ = 0.4 in 1 mL. Two samples of each strain/condition were collected as technical replicates per biological replicate. The cells were washed with 1 mL PBSE (PBS, pH 7.4, 1 mM EDTA) twice, pelleted and frozen at −20 °C until analysis. Each sample was digested in 550 μL 35% trace-metal-free $HNO_3$ (BDH Chemicals) and 50 μL of each neat sample was removed and diluted 1/10 in 35% $HNO_3$. An In-112 standard (5 ppb in 35% $HNO_3$) was run before each set of samples to correct for signal fluctuations in the instrument. The Ni-60 signals were measured from the neat samples and Mg-24 signals from the 1/10 dilutions, because the Mg-24 signal saturated the detector in the neat samples. The raw counts for each isotope were collected as an average of six readings in five sweeps. The Mg-24 signal was used as an internal control to correct the Ni-60 signals for the loss of cells during washing and pipetting.

## Results

### Identifying and analyzing new *Hp*NikR targets

*Hp*NikR is pleiotropic transcription factor that controls a wide repertoire of promoters, and the extent of its activity is not clear. To explore the regulon of *Hp*NikR and discover new targets, chromatin immunoprecipitation sequencing (ChIP-seq) was performed, a method that has been widely used to define the regulatory network of many transcription factors.[43,44] A pilot experiment using *H. pylori* grown at neutral pH in media supplemented with 20 μM nickel revealed known *Hp*NikR targets including *nikR*[22,45,46] and *fecA3*.[22,45–47] Several well-characterized targets such as *ureA*[22,23,27,45,46] were not identified under these experimental conditions, but the reason for this deficiency is not clear. A quantitative Western blot experiment using cell lysates from wild-type *H. pylori* revealed that the *Hp*NikR protein is present in the bacteria at an intracellular concentration of roughly 10 μM (data not shown), so the absence of any confirmed target is not a result of insufficient *Hp*NikR expression.

Several novel promoters were also identified as putative targets of *Hp*NikR (Table S2, ESI†). Two genes identified in this initial experiment are HPG27_1499 and HPG27_866, referred to as 1499 and 866 in this report, which respectively encode CeuE, the periplasmic protein component of a putative transporter of the ABC superfamily[33,34] and FrpB2, an iron-responsive outer membrane protein.[31–33] Both of these genes were identified as possible targets of *Hp*NikR in a previous microarray study of the SS1 strain of *H. pylori*,[45] but direct regulation of these genes by *Hp*NikR has not been demonstrated. Given this precedence, the possibility of nickel-responsive regulation of these genes by *Hp*NikR was explored.

### Nickel-activated *Hp*NikR directly binds to the target promoters

To validate the results of the ChIP-seq experiment, we examined whether *Hp*NikR can bind directly to the two promoter sequences by using electrophoretic mobility shift assays (EMSAs). In the presence of 800 μM $NiSO_4$, *Hp*NikR binds to the 1499 sequence at half-maximal saturation with a protein concentration of 140 nM (Fig. 1, Table 1). Under the same conditions, *Hp*NikR also binds to the 866 promoter with an affinity of approximately 60 nM (Fig. 1, Table 1). In both cases, no visible shift was observed when the experiment was run with 75 μM $NiSO_4$ (data not shown). DNA binding by holo-*Hp*NikR (loaded with 1 : 1 nickel) was also observed when 3 mM $MgSO_4$ was included in the gel and running buffer (Fig. 2). The calculated

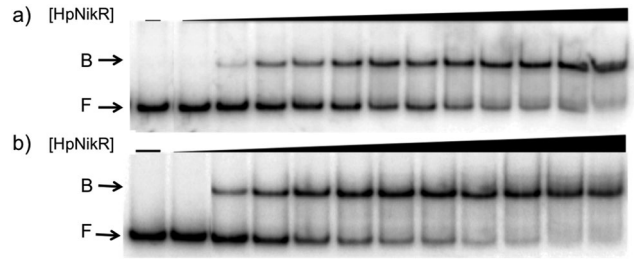


Fig. 1 DNA binding of *Hp*NikR in excess nickel. Oligonucleotides containing the sequence from the HPG27_1499 promoter (a) or the HPG27_866 promoter (b) were incubated with holo-*Hp*NikR (1–600 nM or 0.1 nM to 1 μM, respectively). The reactions were analysed on 6% native polyacrylamide gels with 800 μM $NiSO_4$ in the gel and running buffer. F indicates free DNA and B indicates protein-bound DNA. The data were analysed as described in the Experimental section and the average protein concentrations required for half-maximal saturation are listed in Table 1.

Table 1 Apparent DNA-binding affinities ($\times 10^{-9}$ M)[a]

| | EMSA | | DNase footprint | |
|---|---|---|---|---|
| | Holo-*Hp*NikR | | Holo-*Hp*NikR | Excess Ni(II) |
| | 800 μM $NiSO_4$ | 3 mM $MgSO_4$ | 1 : 1 Ni(II) | 35 μM $NiCl_2$ |
| 1499 | 140 ± 30 | 130 ± 80 | 230 ± 80 | 330 ± 40 |
| Hill coefficient | 1.3 ± 0.3 | 1.9 ± 0.8 | 2.1 ± 0.3 | 2.02 ± 0.04 |
| 866 | 60 ± 50 | 22 ± 5 | 210 ± 70 | N/D |
| Hill coefficient | 1.4 ± 0.2 | 1.9 ± 0.4 | 1.7 ± 0.4 | N/D |

N/D – Not determined. [a] Values are the average protein concentrations required for half-maximal saturation and standard deviation from at least three experiments.

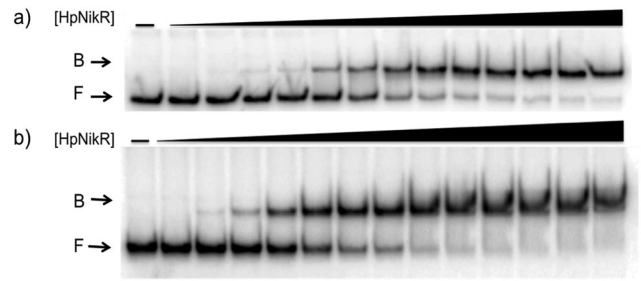


Fig. 2 Magnesium as a requirement of holo-*Hp*NikR for DNA binding. Holo-*Hp*NikR (0.1–600 nM) was incubated with either the 1499 promoter sequence (a) or the 866 promoter sequence (b) and analysed on a 6% native polyacrylamide gel with 3 mM $MgSO_4$ in the gel and running buffer. F indicates free DNA and B indicates protein-bound DNA. The data were analysed as described in the Experimental section and the average protein concentrations required for half-maximal saturation are listed in Table 1.

Ni(II)-*Hp*NikR affinities for the 1499 and 866 sequences that were measured in excess Mg(II) were similar to those measured in excess Ni(II) and revealed that approximately 100 nM protein was required for half-maximal binding on both promoters (Table 1). These results are consistent with previous observations that an excess of divalent cations are required to detect clear DNA binding by nickel-loaded *Hp*NikR.[26,37,48]

In contrast, apo-*Hp*NikR did not interact with either promoter in the presence of 1 mM EDTA, which was added to the gel and buffer to ensure that *Hp*NikR was metal-free (data not shown). Mobility shift assays performed with apo-*Hp*NikR in the presence of 3 mM $MgSO_4$ in the gel and running buffer revealed weak but detectable binding to the 866 and 1499 promoters (Fig. S1, ESI†). Apo-*Hp*NikR binding in the presence of excess Mg(II) was only detected with >50 μM protein, a concentration several orders of magnitude higher than that required for DNA binding by holo-*Hp*NikR.

## Localizing the *Hp*NikR binding site

To locate the binding sites of *Hp*NikR on the 1499 and 866 promoters, DNase I footprinting assays with holo-*Hp*NikR were performed. These assays revealed a 37 bp protected region on the 1499 sequence (Fig. 3) and titration of Ni(II)-*Hp*NikR into the reactions resulted in half-maximal DNA binding with 230 nM protein, comparable to the affinity measured by EMSA. Similarly, a 37 bp footprint was detected on the 866 promoter with a calculated affinity of 210 nM (Fig. 4). Both recognition sequences are AT-rich and loosely follow the pseudo-palindromic consensus sequence (TATTATT-$N_{11}$-AATAATA) proposed by Delany *et al.* (Fig. 5),[28] as well as the modified version suggested by Stoof *et al.* (TRWYA-$N_{15}$-TRWYA).[29] Furthermore, the recognition sequence on the 866 promoter matches the region predicted by bioinformatic analysis of the *frpB2* promoter in *H. pylori* 26695, albeit with some minor changes in the flanking and bridging sequences.[29] Finally, the same footprint region and binding constant were observed when *Hp*NikR was incubated with the 1499 promoter in the presence of excess nickel (Fig. S2, ESI†), which suggests that excess nickel is not required for tight binding of the promoter in this footprinting experiment. Altogether, these results demonstrate that the promoters of 866 and 1499 are directly bound by *Hp*NikR in a nickel-dependent manner.

## *In vivo* regulation of *1499* and *866* by *Hp*NikR

To determine the influence of nickel on the transcription of 1499 and 866 and the role of *Hp*NikR in this response, quantitative PCR (qPCR) was performed. Wild-type *H. pylori* G27 and an isogenic *ΔnikR* strain were grown in the absence or presence of nickel. Two different conditions were applied, either an overnight incubation in media supplemented with 10 μM nickel, or a shorter 15 min exposure to higher nickel concentrations (100 μM). As a positive control for our *in vivo* analysis, *ureA* gene transcription was also examined. The *ureA* gene encodes the large subunit of the *H. pylori* urease enzyme, which is an abundant nickel metalloenzyme in *H. pylori* that is crucial for acid resistance and is a critical virulence factor for *H. pylori* infection.[11,49–51] Upregulation of *ureA* upon nickel exposure has been observed previously, attributed to the activity of *Hp*NikR, and recently it was discovered that *ureA* is among the first genes activated by *Hp*NikR when *H. pylori* are exposed to increased nickel concentrations.[22,23,27,52]

In this study, the qPCR data reveal a statistically significant upregulation of *ureA* upon exposure of wild-type *H. pylori* to 10 μM nickel (Fig. 6), in agreement with previous studies.[22,27,52] No significant difference in *ureA* transcription was detected in the Δ*nikR* strain upon nickel supplementation, consistent with

 

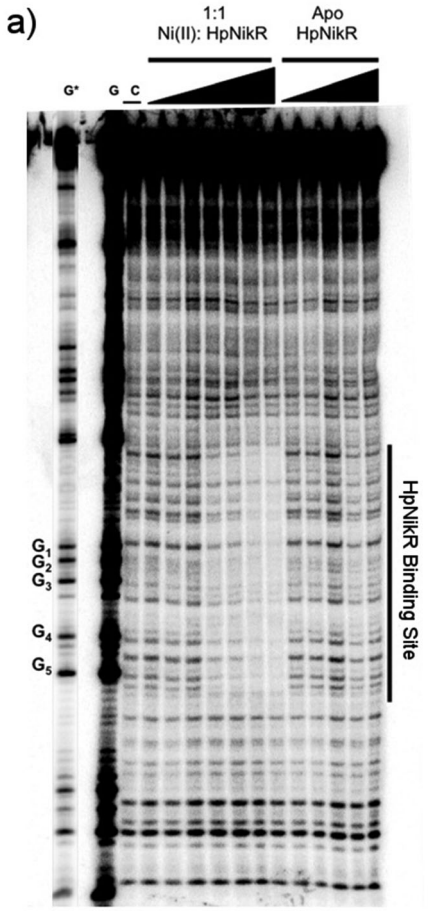


Fig. 3 DNA binding by *Hp*NikR on the 1499 promoter sequence. (a) Apo-*Hp*NikR (50 nM–5 μM) and holo-*Hp*NikR (50 nM–5 μM) were incubated with $^{32}$P-radiolabeled 179 bp DNA probe containing the HPG27_1499 promoter sequence before cleavage with DNase I. The reactions were resolved on an 8% denaturing polyacrylamide gel and the area of protection is indicated. Key: G and G*, Maxam–Gilbert G reaction with longer and shorter reaction times, respectively; C, control DNase I reaction in the absence *Hp*NikR. The apparent DNA-binding affinity, determined to be 230 ± 80 nM with a Hill coefficient of 2.1 ± 0.3, is an average from four independent experiments. (b) DNA sequence of the 1499 promoter. The binding region is underlined and the guanines within the footprint are bolded and noted on the footprint gel. Note that the 1499 probe used is the reverse complement of the genomic promoter sequence, thus the start codon is upstream of the indicated binding site.

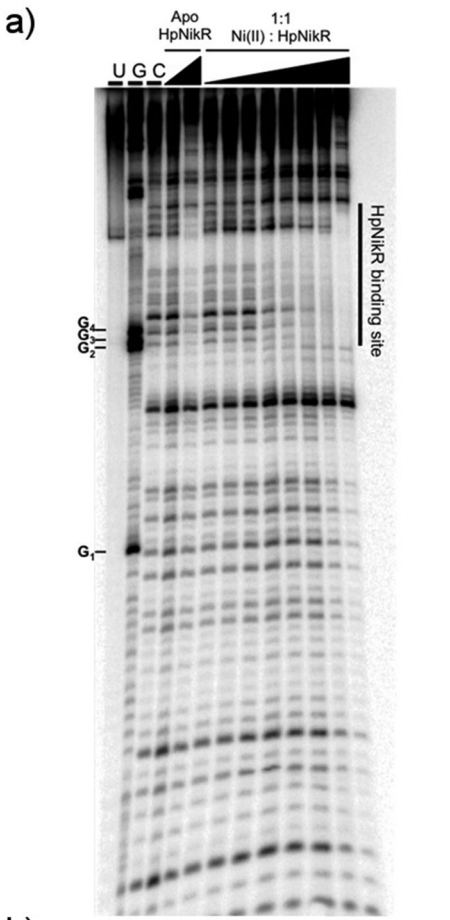


Fig. 4 DNA binding by *Hp*NikR on the 866 promoter. (a) Apo-*Hp*NikR (100 nM, 10 μM) and holo-*Hp*NikR (100 nM–10 μM) were incubated with $^{32}$P-radiolabeled 185 bp DNA probe containing the HPG27_866 promoter sequence prior to the addition of DNase I. The reactions were resolved on an 8% denaturing polyacrylamide gel and the area of protection is indicated. Key: U, undigested 190 bp probe; G, Maxam–Gilbert G reaction; C, control DNase I reaction of 185 bp probe with no *Hp*NikR. The apparent DNA-binding affinity was determined to be 210 ± 70 nM with a Hill coefficient of 1.7 ± 0.4, calculated as an average from three independent experiments. (b) DNA sequence of the 866 promoter region. The binding region is underlined and the guanines within the footprint are bolded and noted on the footprint gel. Note that the 1499 probe used is the reverse complement of the genomic promoter sequence, thus the start codon is upstream of the indicated binding site.

the role of *Hp*NikR as the primary nickel-responsive regulator in the cell. In contrast to the impact on *ureA*, the transcription levels of 866 and 1499 were significantly repressed when the wild-type bacteria were grown in nickel-supplemented media (Fig. 6), whereas no change in expression was observed for either gene when nickel was added to the Δ*nikR* knockout strain. These results suggest that 866 and 1499 are directly regulated by nickel-activated *Hp*NikR, consistent with the *in vitro* DNA-binding data.

Similar trends were observed when the bacteria were grown with higher levels of nickel but for a shorter time (Fig. S3, ESI†). Nickel supplementation results in activation of *ureA* gene

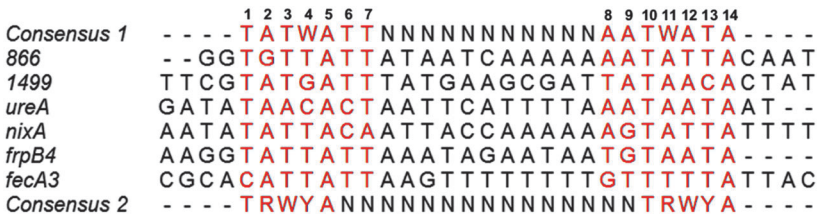


Fig. 5 Alignment of the *Hp*NikR binding sites from select promoters. The two parts of the consensus sequence are bolded, in red, and numbered according to Evans *et al.* for the aligned sequences.[62] Consensus 1 and Consensus 2 represent the DNA recognition sites proposed by Delany *et al.*[28] and Stoof *et al.*,[29] respectively. N represents any nucleotide and W represents either an A or T nucleotide. Clustal Omega was used to align the promoters and generate the image.

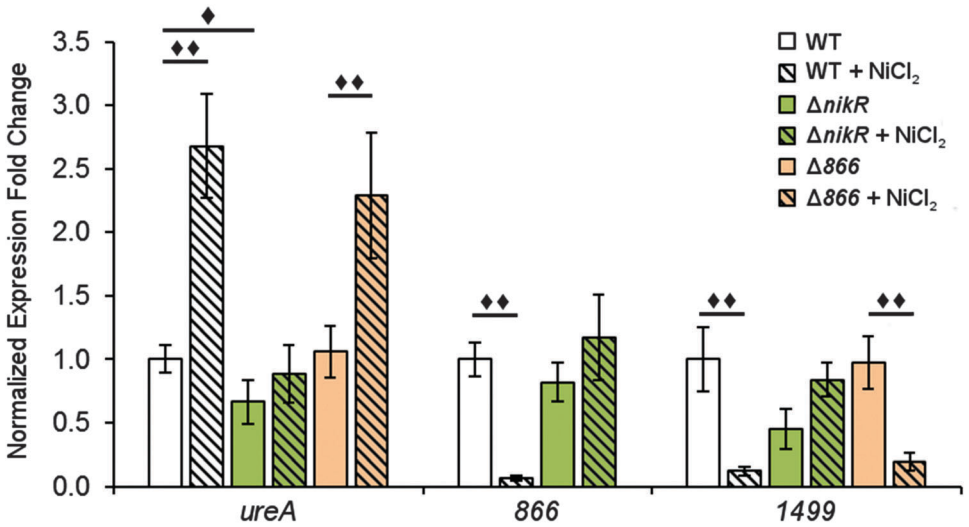


Fig. 6 Expression of *H. pylori* G27 genes after overnight nickel exposure. Quantitative PCR was used to analyse *H. pylori* G27 (wild-type, Δ*nikR* or Δ*866*) grown overnight to midlog phase in the presence or absence of a 10 μM $NiCl_2$ media supplement. Expression of the *ureA*, *866* and *1499* genes were normalized to *16S* and *gyr* expression levels and relative to wild-type expression of the gene in the absence of supplemental nickel. Statistically significant differences are represented by diamonds (◆ = $P < 0.05$, ◆◆ = $P < 0.01$). All data represent the average values from at least three biological replicates with three technical replicates each and error bars represent one standard error of the mean.

transcription and repression of the 866 and 1499 genes in the wild-type strain. A small but significant reduction in *ureA* expression was observed in Δ*nikR* strain under these growth conditions, and while this latter observation could suggest a nickel-responsive component in *ureA* regulation that is not directly controlled by *Hp*NikR, as previously suggested,[22] the exact physiological basis behind this effect is not known. In addition, under the short exposure conditions, 1499 transcription was upregulated in the Δ*nikR* strain *versus* the wild-type strain when grown in unsupplemented media. One possible explanation is that apo-*Hp*NikR is regulating 1499 *in vivo*, but this model is not consistent with the extremely weak DNA binding observed *in vitro* with apo-*Hp*NikR on the 1499 promoter. Instead, it is more likely that trace levels of holo-*Hp*NikR cause some repression, which is alleviated in the knock-out strain, or that the 50 mM urea added to the cultures for the short exposures affected relative transcription levels, as urea was previously observed to affect global transcription levels in *H. pylori*.[53]

There is evidence for overlap between the *Hp*NikR and *Hp*Fur regulons.[18,28] Furthermore, both 866 and 1499 are regulated in an iron-responsive fashion in some strains,[32,33,35] but not in others,[54–56] so iron-mediated regulation was also investigated in this study (Fig. 7). No significant change was observed in *ureA* transcription when either the wild-type or Δ*nikR G27* bacteria were exposed to iron-supplemented media, in agreement with previous reports.[52,55] Similarly, the expression of 866 was unaffected by iron. In contrast, the expression of 1499 was observed to increase significantly in wild-type *H. pylori* when the bacteria were exposed to $FeCl_3$. This effect was not observed with the *ΔnikR* mutant, suggesting that the iron-dependent component of 1499 regulation may be mediated through *Hp*NikR.

### Metal uptake through HPG27_866

Given the nickel-responsive regulation of 866, we examined the effects of an 866 knockout on gene transcription and nickel uptake by *H. pylori* G27. The Δ866 strain did not exhibit any significant changes in the growth rate *versus* the wild type, with or without nickel supplementation of the media (data not shown), suggesting that 866 is not critical for *H. pylori* growth under standard laboratory conditions. Furthermore, the baseline and nickel-dependent regulation of *ureA* and 1499

 

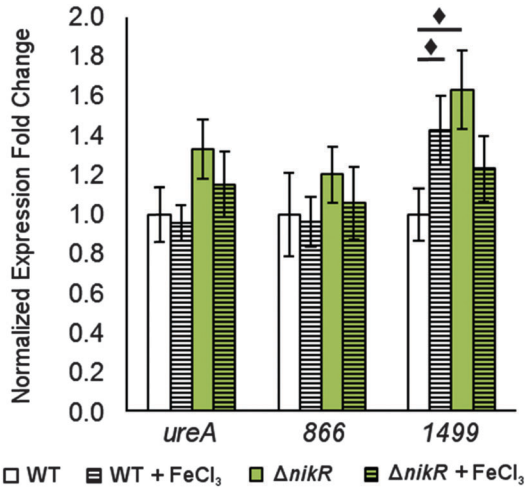


Fig. 7 Changes in gene expression in response to transient iron exposure. Quantitative PCR for *H. pylori* G27 and its isogenic *ΔnikR* mutant grown to mid-log phase and exposed to 100 μM $FeCl_3$ for 30 minutes. Fold expression is relative to *16S* and *gyr* expression under the same conditions and normalized to WT without supplemented metal. Statistically significant differences between expression levels ($P < 0.05$) are marked with a diamond. The data represent the average values from at least three independent biological and technical replicates, and the error bars indicate one standard deviation.

transcription were not significantly different in the Δ866 strain *versus* the wild-type bacteria (Fig. 6), suggesting that any impact of 866 is insufficient to influence the activity of *Hp*NikR.

To directly observe changes in metal uptake as a result of 866 gene expression, total nickel levels in the wild-type, Δ*nikR* and Δ866 *H. pylori* were compared by using inductively-coupled plasma mass spectrometry (ICP-MS, Fig. 8).[15,33,57] Under standard growth conditions, nickel accumulation in the Δ*nikR* strain increased 1.4-fold relative to the wild-type, consistent with previous experiments with an *H. hepaticus* Δ*nikR* strain.[58] *Hp*NikR operates in a negative feedback loop to downregulate nickel import into the cell by repressing the transcription of several nickel uptake genes in a nickel-dependent manner.[18,19] Therefore, the lack of this *Hp*NikR-mediated nickel homeostasis could account for the relative increase in nickel in the Δ*nikR* strain. In contrast, total nickel was significantly lower in the Δ866 strain *versus* the wild type (Fig. 8), demonstrating that this transporter does influence nickel accumulation. Furthermore, the amounts of $^{59}Co$, $^{63}Cu$ and $^{64}Zn$ were not significantly different between the three strains (data not shown). The levels of $^{56}Fe$ could not be accurately measured because of interference from atmospheric argon.[59] Nickel accumulation was also examined in bacteria grown in nickel-supplemented media. Under these conditions, the total nickel content increased markedly in all three strains, and again there was a relative increase in the Δ*nikR* strain compared with the wild-type bacteria, but no significant difference was detected in the Δ866 strain.

## Discussion

*H. pylori* requires a reliable supply of nickel to activate several enzymes that are critical for colonization, and nickel uptake and distribution is primarily regulated by the pleiotropic transcriptional regulator *Hp*NikR (Fig. 9).[23,45] Given the extensive network of nickel homeostasis factors in this organism,[14,16,18] as well as the unusually low number of annotated transcription factors in the *H. pylori* genome compared with similar bacteria,[60] it is perhaps not surprising that *Hp*NikR has such expansive responsibilities and as such, it has been dubbed a master regulator. However, it is not clear how broadly *Hp*NikR exerts its control, so we initiated a search for new nickel-regulated *Hp*NikR targets to provide insight into the mechanism of action of *Hp*NikR in *H. pylori*.

Our pilot ChIP-sequencing experiment revealed the HPG27_866 and HPG27_1499 genes encoding the iron-responsive outer membrane protein FrpB2 and the nickel-binding periplasmic protein CeuE, respectively. These genes were previously implicated as possible targets of *Hp*NikR *via* a microarray study,[45] but given

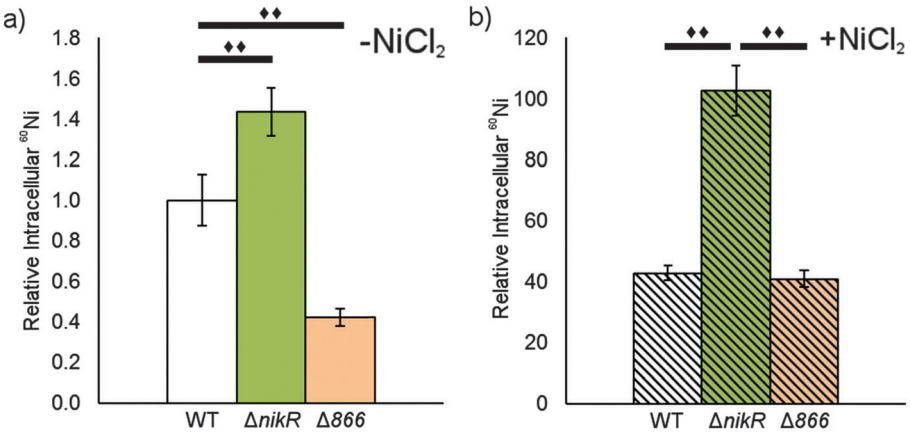


Fig. 8 The impact of HPG27_866 on total nickel. The levels of total cellular nickel was measures in wild-type, Δ*nikR* and Δ*866 H. pylori* G27 using ICP-MS. Each strain was grown overnight without (a) or with (b) a media supplement of 10 μM $NiCl_2$. Counts from $^{24}Mg$ were used as an internal control for differences in cell number for each sample. The data represent the average values from five biological replicates and significant changes ($P < 0.01$) between conditions are marked with a double diamond.

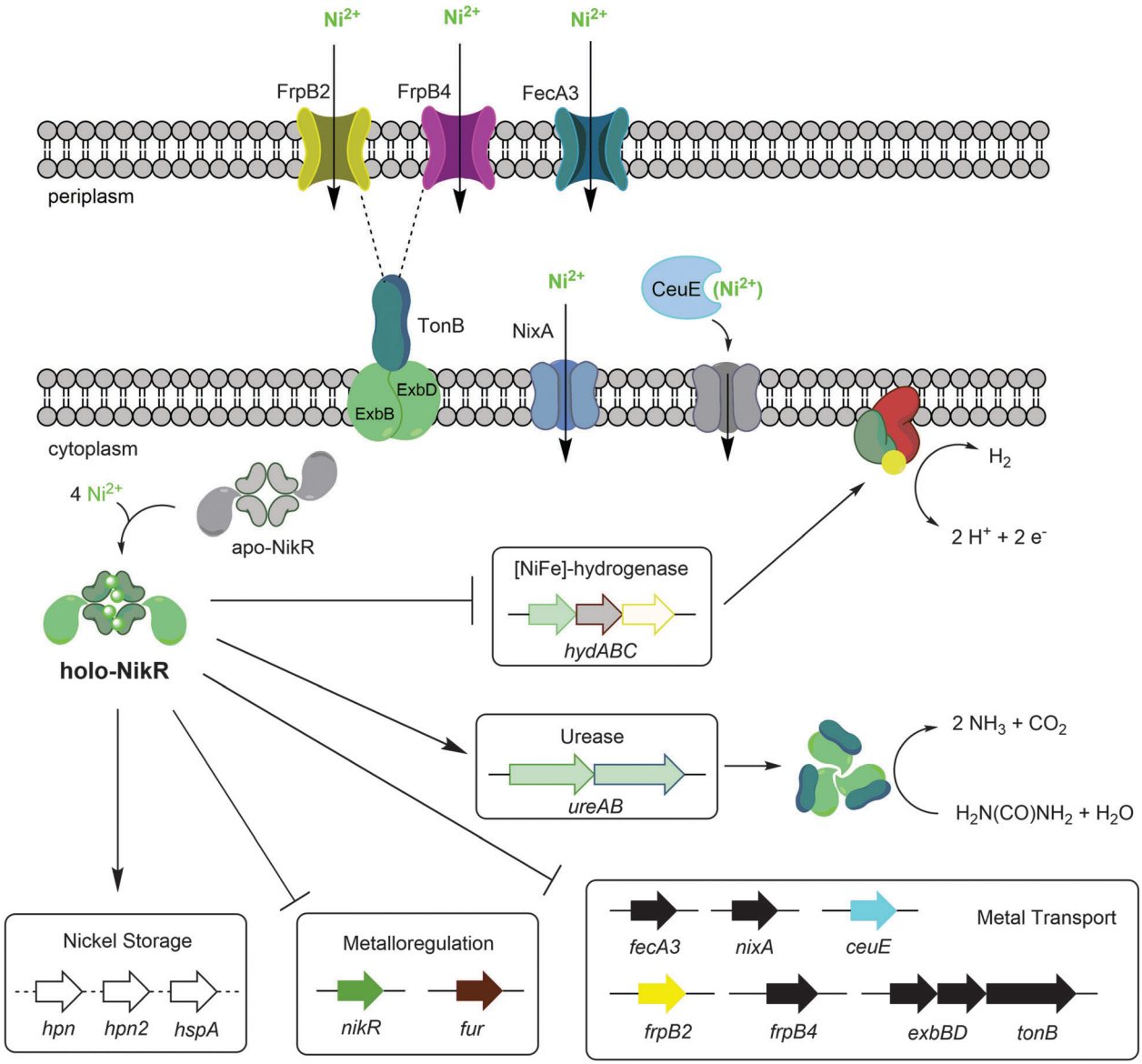


Fig. 9 Regulation by Ni(II)-*Hp*NikR *in vivo*. The transmembrane components of the CeuE nickel transporter have not been explicitly defined, although there is some evidence that FecD/FecE fill these roles. The TonB–ExbB–ExbD complex is believed to provide energy to the FrpB2 outer membrane protein,[33] and may also power the FrpB4 homolog as well. Note that although urease is depicted as a cytoplasmic protein, it is present in the cytoplasm, outer membrane and is also excreted outside the cell.[72] The exact nature of the nickel transported is not clear for all systems, and only genes regulated by *Hp*NikR in response to nickel are shown.

that direct regulation of these genes by *Hp*NikR had not been demonstrated and that the ChIP-seq strategy tends to produce false positives through non-specific binding,[61] we examined whether *Hp*NikR regulates these two genes in response to nickel. *In vitro* DNA-binding assays were used to demonstrate nickel-responsive *Hp*NikR binding to both promoter sequences, the recognition sequences were mapped out, and *in vivo* transcriptional analysis indicated that *Hp*NikR represses transcription of both genes in response to an increase in the levels of environmental nickel. Altogether, these results suggest that both 866 and 1499 are components of the *Hp*NikR regulon.

Analysis of the Ni(II)-*Hp*NikR–DNA complexes by using both EMSAs and DNAse footprinting assays revealed half-maximal saturation with ~100 nM protein on the promoter sequences of both HPG27_866 and HPG27_1499, a value comparable to the affinities of *Hp*NikR for other DNA recognition sites.[20,21,26,37,48] Some *Hp*NikR–DNA complexes are significantly weaker, and it was proposed that the promoters regulated by *Hp*NikR can be divided into two classes, with the tighter complexes being observed for the genes that encode proteins that directly utilize nickel ($K_d$ values of low-to-mid nM) and weaker complexes on the promoters of genes of other types of proteins ($K_d$ values of low μM and weaker).[20] The affinity of *Hp*NikR for 866 and 1499 promoter sequences places these genes in the former class, along with the genes encoding other nickel membrane transporters as well as urease. However, it is unclear how this

 

two-tiered mode of recognition observed by the *in vitro* studies translates into the physiological activity of *Hp*NikR.[22]

DNase footprinting assays revealed that the sequences of the *Hp*NikR binding sites on the 866 and 1499 promoters are 37 bp, AT-rich sequences (Fig. 5). Although neither is an exact match for the initially proposed consensus sequence TATTATT-$N_{11}$-AATTATA,[28] some resemblance is clear, and the 866 site is in full agreement with the more inclusive and recently derived version TRWYA-$N_{15}$-TRWYA.[29] This newer version of the *Hp*NikR consensus was generated by analysing known NikR binding sites from several *Helicobacter* species. It was then applied to predict NikR targets in *Helicobacter* genomes, and one of the operators identified was that of the 866 analog in *H. pylori* 26695, *frpB2* (HP0916) (Fig. S4, ESI†).[29] It has also been suggested that several specific DNA bases in the *Hp*NikR recognition sequences are more crucial for protein binding than others, with thymine 10 at the 3' half-site serving a role in distinguishing the tight binders from the weak ones.[62] In support of this proposal, both the 1499 and 866 recognition sequences have thymine at position 10, consistent with the relatively tighter affinity of these *Hp*NikR–DNA complexes.

In the *H. pylori* strain 26695, the gene orthologous to 866 is split by a stop codon caused by a frame-shift deletion, forming *frpB2* and the pseudogene *frpB3* (HP0916 and HP0915, respectively), which are repressed by the iron metalloregulator *Hp*Fur in an iron-dependent manner.[32] However, iron-responsive regulation of this gene is not always observed. Iron-dependent changes in 866 expression were not observed in the G27 wild-type or Δ*nikR* strains under the conditions used in this study, a result consistent with previous experiments with *H. pylori* G27[54] as well as with array-based studies of other strains.[35,55] Furthermore, neither of the promoters of HPG27_866 and HP0916/HP0915 contain the putative *Hp*Fur recognition sequence and evidence that *Hp*Fur binds directly to these promoters is lacking.[54,63] In contrast, the promoters in both strains contain a *Hp*NikR binding site (as observed in this work and previously[29]), albeit with slight variations in the bridging and flanking sequences of each (Fig. S4, ESI†), and the *in vitro* and *in vivo* experiments reported here demonstrate that regulation of this gene is directly controlled by *Hp*NikR in response to nickel. Although iron-responsive regulation of 866 is not consistently observed, it is possible that *frpB2* expression is modulated indirectly by iron under some conditions through *Hp*NikR activity. It has been previously suggested that the *Hp*NikR and *Hp*Fur regulons overlap;[18,28] for example both proteins have been demonstrated to directly regulate common genes such as the *hydABC* cassette[22,63] and *Hp*NikR directly represses the transcription of *Hp*Fur.[20,22]

Deletion of HPG27_866 negatively affects nickel accumulation in *H. pylori* grown under standard laboratory conditions, suggesting that this outer membrane transporter may be involved in nickel uptake. No significant impact was observed on the expression of the *ureA* or 1499 genes in the Δ*866* mutant strain, indicating that *Hp*NikR activity is not affected. The lack of impact on regulation despite lower nickel levels could arise from partitioned pools of nickel within *H. pylori*, as proposed for *E. coli*.[64] It has also been suggested that FrpB2 contributes to iron uptake as a haemoglobin receptor. Overexpression of the FrpB2 protein encoded by *H. pylori* J99 allows *E. coli* to survive in an iron-deficient medium that was supplemented with Hb, and analysis of the crude *E. coli* lysates suggested that FrpB2 could bind human haemoglobin.[31] A connection between nickel and heme uptake was also made with the observation that *E. coli* NikA, the periplasmic component of the NikABC transporter, can bind heme,[65] although how this activity contributes to heme utilization is not clear.[66] Future work on the biochemistry and cell biology of FrpB2 will be necessary to pinpoint the specific role that it plays in metal uptake in *H. pylori*.

HPG27_1499 was also originally annotated as an iron transport protein, possibly due to the homology with the *Campylobacter coli* periplasmic iron-binding protein.[67,68] Despite the weak binding affinity of *Hp*Fur to the 1499 binding site,[56] iron-responsive regulation of the corresponding gene in *H. pylori* SS1 was observed only in the stationary growth phase and not in other strains.[32,35,55,56] Furthermore, mutation of the genes encoding the putative transmembrane components of this ABC transporter, *fecD* and *fecE*, did not dramatically impact the iron uptake in *H. pylori* 11637,[67] suggesting that this transporter is involved in the uptake of a different metal. In this study, weak but significant upregulation of HPG27_1499 was observed upon a brief exposure to high concentrations of iron in the wild-type bacteria ($P = 0.049$) but not in the Δ*nikR* mutant strain. As discussed above for HPG27_866, it is possible that iron-responsive regulation of HPG27_1499 is a result of cross-regulation between *Hp*Fur and *Hp*NikR. As previously suggested, the sigma factor RpoD ($\sigma^{80}$) could also be affecting the transcription of 1499 through an unknown indirect iron-dependent pathway.[69] While not yet validated, the *rpoD* gene was identified as a putative target of *Hp*NikR by our ChIP-seq results and contains the *Hp*NikR consensus binding sequence in its promoter, but further experiments would be required to test this hypothesis.

The assignment of HPG27_1499 as a component of the *Hp*NikR regulon is consistent with the recent re-classification of this protein as a factor involved in nickel acquisition. Interruption of the corresponding *ceuE* or *fecD* genes in *H. mustelae* resulted in decreased total nickel and cobalt.[33] Furthermore, recent structural analysis of *H. pylori* CeuE revealed that it matches the fold of a periplasmic-binding-protein component of an ABC metal transporter and that it binds Ni(L-His)$_2$, similar to *E. coli* NikA,[70] but not heme, vitamin B12 or enterobactin.[34] These observations suggest a model for a biological connection between *Hp*NikR and CeuE that is analogous to *E. coli* NikR and the NikABCDE inner membrane nickel transporter, where *Hp*NikR represses transcription of CeuE to halt nickel import in response to high concentrations of extracellular nickel.[19,71] The genes encoding FecD and FecE, HPG27_842 and HPG27_841, respectively, are in a separate operon from 1499 and seemingly lack an *Hp*NikR recognition sequence in the promoter region. However, the *fecE* gene was also identified as an HpNikR target in our ChIP-Seq data

(Table S2, ESI†), suggesting that the transmembrane and periplasmic components of the CeuE/FecD/FecE transporter could be regulated by *Hp*NikR in concert.

## Conclusions

Ni(II)-*Hp*NikR binds to the promoters of HPG27_1499 (*ceuE*) and HPG27_866 (*frpB2*) *in vitro* with strong, sub-micromolar binding affinities, and DNase I footprinting revealed binding sites within both promoters that resemble the established pseudo consensus sequences. Furthermore, the transcription of both genes is significantly downregulated when *H. pylori* is exposed to media supplemented with $NiCl_2$, a response that is dependent on the presence of *Hp*NikR, linking the *in vivo* transcription of 866 and 1499 to the *H. pylori* nickel response. These results allow these genes to be assigned to the *Hp*NikR regulon, and the impact of the 866 deletion on nickel accumulation is consistent with a role of the gene product in nickel transport. Future work will establish the mechanism of how these proteins contribute to metal homeostasis in *H. pylori*. Finally, these experiments provide a snapshot of the *Hp*NikR regulon under a single set of growth conditions, but it is clear that multiple variables impact the activity of this protein, including time and pH.[21,22,24,25] Analysis of bacteria exposed to different conditions will provide details of how HpNikR supports *H. pylori* as it adapts to the challenges of its niche environment.

## Acknowledgements

The authors would like to thank Dr Lisa Willis for her advice on the construction of *H. pylori* knockouts. This work was supported in part by funding from the Natural Sciences and Engineering Research Council (NSERC) of Canada and the Canadian Institutes of Health Research. M.D.J. is partially funded through an Ontario Graduate Scholarship.

## Notes and references

1 Y. Li and D. B. Zamble, *Chem. Rev.*, 2009, **109**, 4617–4643.
2 S. W. Ragsdale, *J. Biol. Chem.*, 2009, **284**, 18571–18575.
3 J. L. Boer, S. B. Mulrooney and R. P. Hausinger, *Arch. Biochem. Biophys.*, 2014, **544**, 142–152.
4 J. S. Williamson, *Curr. Pharm. Des.*, 2001, **7**, 355–392.
5 B. E. Dunn, H. Cohen and M. J. Blaser, *Clin. Microbiol. Rev.*, 1997, **10**, 720–741.
6 M. Sibony and N. L. Jones, *Curr. Opin. Gastroenterol.*, 2012, **28**, 30–35.
7 G. Sachs, D. L. Weeks, K. Melchers and D. R. Scott, *Annu. Rev. Physiol.*, 2003, **65**, 349–369.
8 K. Stingl, E. M. Uhlemann Em, G. Deckers-Hebestreit, R. Schmid, E. P. Bakker and K. Altendorf, *Infect. Immun.*, 2001, **69**, 1178–1180.
9 D. R. Scott, E. A. Marcus, Y. Wen, J. Oh and G. Sachs, *Proc. Natl. Acad. Sci. U. S. A.*, 2007, **104**, 7235–7240.
10 S. B. Mulrooney and R. P. Hausinger, *FEMS Microbiol. Rev.*, 2003, **27**, 239–261.
11 M. Pflock, S. Kennard, N. Finsterer and D. Beier, *J. Biotechnol.*, 2006, **126**, 52–60.
12 W. Fischer, S. Prassl and R. Haas, in *Molecular Mechanisms of Bacterial Infection via the Gut*, ed. C. Sasakawa, Springer-Verlag, Berlin, Heidelberg, 2009, pp. 129–171.
13 J. W. Olson and R. J. Maier, *Science*, 2002, **298**, 1788–1790.
14 R. J. Maier, S. L. Benoit and S. Seshadri, *BioMetals*, 2007, **20**, 655–664.
15 K. Schauer, C. Muller, M. Carriere, A. Labigne, C. Cavazza and H. De Reuse, *J. Bacteriol.*, 2010, **192**, 1231–1237.
16 C. Belzer, J. Stoof and A. H. van Vliet, *BioMetals*, 2007, **20**, 417–429.
17 J. M. Whitmire, H. Gancz and D. S. Merrell, *Curr. Med. Chem.*, 2007, **14**, 469–478.
18 A. Danielli and V. Scarlato, *FEMS Microbiol. Rev.*, 2010, **34**, 738–752.
19 M. D. Jones, A. M. Sydor and D. B. Zamble, in *Metals in Cells*, ed. R. S. Scott and V. Culotta, John Wiley & Sons, Ltd, New York, 2013, pp. 277–288.
20 N. S. Dosanjh, A. L. West and S. L. J. Michel, *Biochemistry*, 2009, **48**, 527–536.
21 Y. Li and D. B. Zamble, *Biochemistry*, 2009, **48**, 2486–2496.
22 C. Muller, C. Bahlawane, S. Auber, C. M. Delay, K. Schauer, I. Michaud-Soret and H. De Reuse, *Nucleic Acids Res.*, 2011, **39**, 7564–7575.
23 A. H. van Vliet, S. W. Poppelaars, B. J. Davies, J. Stoof, S. Bereswill, M. Kist, C. W. Penn, E. J. Kuipers and J. G. Kusters, *Infect. Immun.*, 2002, **70**, 2846–2852.
24 A. H. van Vliet, F. D. Ernst and J. G. Kusters, *Trends Microbiol.*, 2004, **12**, 489–494.
25 S. Bury-Moné, J. M. Thiberge, M. Contreras, A. Maitournam, A. Labigne and H. De Reuse, *Mol. Microbiol.*, 2004, **53**, 623–638.
26 E. L. Benanti and P. T. Chivers, *J. Biol. Chem.*, 2007, **282**, 20365–20375.
27 F. D. Ernst, E. J. Kuipers, A. Heijens, R. Sarwari, J. Stoof, C. W. Penn, J. G. Kusters and A. H. M. van Vliet, *Infect. Immun.*, 2005, **73**, 7252–7258.
28 I. Delany, R. Ieva, A. Soragni, M. Hilleringmann, R. Rappuoli and V. Scarlato, *J. Bacteriol.*, 2005, **187**, 7703–7715.
29 J. Stoof, E. Kuipers and A. van Vliet, *BioMetals*, 2010, **23**, 145–159.
30 E. L. Benanti and P. T. Chivers, *J. Biol. Chem.*, 2011, **286**, 15728–15737.
31 M. A. González-López and J. J. Olivares-Trejo, *BioMetals*, 2009, **22**, 889–894.
32 A. H. M. Van Vliet, J. Stoof, R. Vlasblom, S. A. Wainwright, N. J. Hughes, D. J. Kelly, S. Bereswill, J. J. E. Bijlsma, T. Hoogenboezem, C. M. J. E. Vandenbroucke-Grauls, M. Kist, E. J. Kuipers and J. G. Kusters, *Helicobacter*, 2002, **7**, 237–244.
33 J. Stoof, E. J. Kuipers, G. Klaver and A. H. M. van Vliet, *Infect. Immun.*, 2010, **78**, 4261–4267.
34 M. M. Shaik, L. Cendron, M. Salamina, M. Ruzzene and G. Zanotti, *Mol. Microbiol.*, 2014, **91**, 724–735.

 

35 D. S. Merrell, L. J. Thompson, C. C. Kim, H. Mitchell, L. S. Tompkins, A. Lee and S. Falkow, *Infect. Immun.*, 2003, **71**, 6510–6525.
36 E. L. Benanti and P. T. Chivers, *J. Bacteriol.*, 2009, **191**, 2405–2408.
37 L. O. Abraham, Y. Li and D. B. Zamble, *J. Inorg. Biochem.*, 2006, **100**, 1005–1014.
38 A. M. Maxam and W. Gilbert, *Proc. Natl. Acad. Sci. U. S. A.*, 1977, **74**, 560–564.
39 J. Sambrook and D. W. Russell, *Molecular Cloning: A laboratory Manual*, Cold Spring Harbor Press, Cold Spring Harbor, New York, 3rd edn, 2001, vol. 2.
40 D. E. Smith and P. A. Fisher, *J. Cell Biol.*, 1984, **99**, 20–28.
41 R. Jothi, S. Cuddapah, A. Barski, K. Cui and K. Zhao, *Nucleic Acids Res.*, 2008, **36**, 5221–5231.
42 R. Haas, T. F. Meyer and J. P. M. van Putten, *Mol. Microbiol.*, 1993, **8**, 753–760.
43 P. J. Franham, *Nat. Rev. Genet.*, 2009, **10**, 605–616.
44 E. R. Mardis, *Nat. Methods*, 2007, **4**, 613–614.
45 M. Contreras, J. Thilberge, M. Mandrand-Berthelot and A. Labigne, *Mol. Microbiol.*, 2003, **49**, 947–963.
46 G. S. Davis, E. L. Flannery and H. L. T. Mobley, *Infect. Immun.*, 2006, **74**, 6811–6820.
47 F. D. Ernst, J. Stoof, W. M. Horrevoets, E. J. Kuipers, J. G. Kusters and A. H. van Vliet, *Infect. Immun.*, 2006, **74**, 6821–6828.
48 N. S. Dosanjh, N. A. Hammerbacher and S. L. J. Michel, *Biochemistry*, 2007, **46**, 2520–2529.
49 B. E. Dunn, G. P. Campbell, G. I. Perez-Perez and M. J. Blaser, *J. Biol. Chem.*, 1990, **265**, 9464–9469.
50 L. T. Hu and H. L. Mobley, *Infect. Immun.*, 1990, **58**, 992–998.
51 K. A. Eaton, C. L. Brooks, D. R. Morgan and S. Krakowka, *Infect. Immun.*, 1991, **59**, 2470–2475.
52 A. H. van Vliet, E. J. Kuipers, B. Waidner, B. J. Davies, N. de Vries, C. W. Penn, C. M. Vandenbroucke-Grauls, M. Kist, S. Bereswill and J. G. Kusters, *Infect. Immun.*, 2001, **69**, 4891–4897.
53 Y. Wen, E. A. Marcus, U. Matrubutham, M. A. Gleeson, D. R. Scott and G. Sachs, *Infect. Immun.*, 2003, **71**, 5921–5939.
54 O. Q. Pich, B. M. Carpenter, J. J. Gilbreath and D. S. Merrell, *Mol. Microbiol.*, 2012, **84**, 921–941.
55 F. D. Ernst, S. Bereswill, B. Waidner, J. Stoof, U. Mader, J. G. Kusters, E. J. Kuipers, M. Kist, A. H. van Vliet and G. Homuth, *Microbiology*, 2005, **151**, 533–546.
56 I. Delany, A. B. F. Pacheco, G. Spohn, R. Rappuoli and V. Scarlato, *J. Bacteriol.*, 2001, **183**, 4932–4937.
57 C. E. Outten and T. V. O'Halloran, *Science*, 2001, **292**, 2488–2492.
58 S. L. Benoit, S. Seshadri, R. Lamichhane-Khadka and R. J. Maier, *Microbiology*, 2013, **159**, 136–146.
59 J. R. Dean, *Practical Inductively Coupled Plasma Spectroscopy*, John Wiley & Sons, Ltd, New York, 2005, pp. 89–122.
60 V. Scarlato, I. Delany, G. Spohn and D. Beier, *Int. J. Med. Microbiol.*, 2001, **291**, 107–117.
61 P. J. Park, *Nat. Rev. Genet.*, 2009, **10**, 669–680.
62 S. E. Evans and S. L. J. Michel, *Dalton Trans.*, 2012, **41**, 7946–7951.
63 B. M. Carpenter, J. J. Gilbreath, O. Q. Pich, A. M. McKelvey, E. L. Maynard, Z.-Z. Li and D. S. Merrell, *J. Bacteriol.*, 2013, **195**, 5526–5539.
64 J. S. Iwig, J. L. Rowe and P. T. Chivers, *Mol. Microbiol.*, 2006, **62**, 252–262.
65 M. Shepherd, M. D. Heath and R. K. Poole, *Biochemistry*, 2007, **46**, 5030–5037.
66 S. Létoffé, P. Delepelaire and C. Wandersman, *Proc. Natl. Acad. Sci. U. S. A.*, 2006, **103**, 12891–12896.
67 J. Velayudhan, N. J. Hughes, A. A. McColm, J. Bagshaw, C. L. Clayton, S. C. Andrews and D. J. Kelly, *Mol. Microbiol.*, 2000, **37**, 274–286.
68 E. Gasteiger, A. Gattiker, C. Hoogland, I. Ivanyi, R. D. Appel and A. Bairoch, *Nucleic Acids Res.*, 2003, **31**, 3784–3788.
69 D. Beier, G. Spohn, R. Rappuoli and V. Scarlato, *Mol. Microbiol.*, 1998, **30**, 121–134.
70 P. T. Chivers, E. L. Benanti, V. Heil-Chapdelaine, J. S. Iwig and J. L. Rowe, *Metallomics*, 2012, **4**, 1043–1050.
71 P. T. Chivers and R. T. Sauer, *J. Biol. Chem.*, 2000, **275**, 19735–19741.
72 P. R. Hawtin, A. R. Stacey and D. G. Newell, *J. Gen. Microbiol.*, 1990, **136**, 1995–2000.